Eur. Phys. J. C (2005)
Digital Object Identifier (DOI) 10.1140/epjc/s2005-02246-5

THE EUROPEAN PHYSICAL JOURNAL C

High-p_T results from PHOBOS

The PHOBOS Collaboration

G. Roland[4,a], B.B. Back[1], M.D. Baker[2], M. Ballintijn[4], D.S. Barton[2], R.R. Betts[6], A.A. Bickley[7], R. Bindel[7], W. Busza[4], A. Carroll[2], Z. Chai[2], M.P. Decowski[4], E. García[6], T. Gburek[3], N. George[2], K. Gulbrandsen[4], C. Halliwell[6], J. Hamblen[8], M. Hauer[2], C. Henderson[4], D.J. Hofman[6], R.S. Hollis[6], R. Hołyński[3], B. Holzman[2], A. Iordanova[6], E. Johnson[8], J.L. Kane[4], N. Khan[8], P. Kulinich[4], C.M. Kuo[5], W.T. Lin[5], S. Manly[8], A.C. Mignerey[7], R. Nouicer[2,6], A. Olszewski[3], R. Pak[2], C. Reed[4], J. Sagerer[6], H. Seals[2], I. Sedykh[2], C.E. Smith[6], M.A. Stankiewicz[2], P. Steinberg[2], G.S.F. Stephans[4], A. Sukhanov[2], M.B. Tonjes[7], A. Trzupek[3], C. Vale[4], G.J. van Nieuwenhuizen[4], S.S. Vaurynovich[4], R. Verdier[4], G.I. Veres[4], E. Wenger[4], F.L.H. Wolfs[8], B. Wosiek[3], K. Woźniak[3], B. Wysłouch[4]

[1] Argonne National Laboratory, Argonne, IL 60439-4843, USA
[2] Brookhaven National Laboratory, Upton, NY 11973-5000, USA
[3] Institute of Nuclear Physics PAN, Kraków, Poland
[4] Massachusetts Institute of Technology, Cambridge, MA 02139-4307, USA
[5] National Central University, Chung-Li, Taiwan
[6] University of Illinois at Chicago, Chicago, IL 60607-7059, USA
[7] University of Maryland, College Park, MD 20742, USA
[8] University of Rochester, Rochester, NY 14627, USA

Received: 18 February 2005 / Revised version: 14 March 2005 /
Published online: 5 August 2005 –

Abstract. We present results from the PHOBOS experiment on charged hadron production over a large range in p_{T}, from Data from d+Au collisions at $\sqrt{s_{NN}} = 200$ GeV and Au+Au collisions at $\sqrt{s_{NN}} = 62.4$ and 200 GeV are shown. The data indicate that in Au+Au collisions a strongly interacting state of matter is formed, that appears qualitatively different from the system formed in pp or d+Au collisions. The systematics of particle production in d+Au and Au+Au collisions exhibit remarkably simple scaling rules, including an apparent factorization of the energy and centrality dependence over a wide range of collision energies.

PACS. 25.75.-q, 25.75.Dw, 25.75.Gz

1 Introduction

The systematic survey of ultra-relativistic heavy ion collisions over a wide range of collision energy and system size has revealed many, sometimes unexpected, properties of strongly interacting matter under extreme conditions: at sufficiently high energies a dense, interacting medium is formed early on in the collision process (see [1] and references therein). In this paper we will show some of the PHOBOS results that contributed to establishing these conclusions. We will also discuss scaling rules that seem to hold over a large range in collision energy and centrality and that have not yet found an explanation in terms of dynamical models of the collision process. A more complete overview of PHOBOS results can be found in [1].

2 Charged hadron spectra in d+Au and Au+Au at $\sqrt{s_{NN}} = 200$ GeV

One of the key pieces of evidence for the creation of a strongly interacting state of matter in heavy-ion collisions at RHIC is the suppression of the yield of high-p_{T} hadrons in Au+Au collisions, relative to expectations based on scaling yields in pp collisions with N_{coll}, the number of binary nucleon+nucleon collisions in a Au+Au collision [2]. This modification of the yield and momentum distribution of particles resulting from initial hard scattering processes has been called "jet quenching". The effect was predicted as the result of energy loss of high momentum partons in the dense medium created early in a heavy-ion collision [3]. This phenomenon has been proposed as a diagnostic tool for characterizing the parton density in the initial stage of high-energy nuclear collisions.

The first results on high-p_{T} spectra at RHIC left open the question whether the observed effect is indeed related to the presence of "matter" in the final state, or related to

[a] e-mail: rolandg@mit.edu

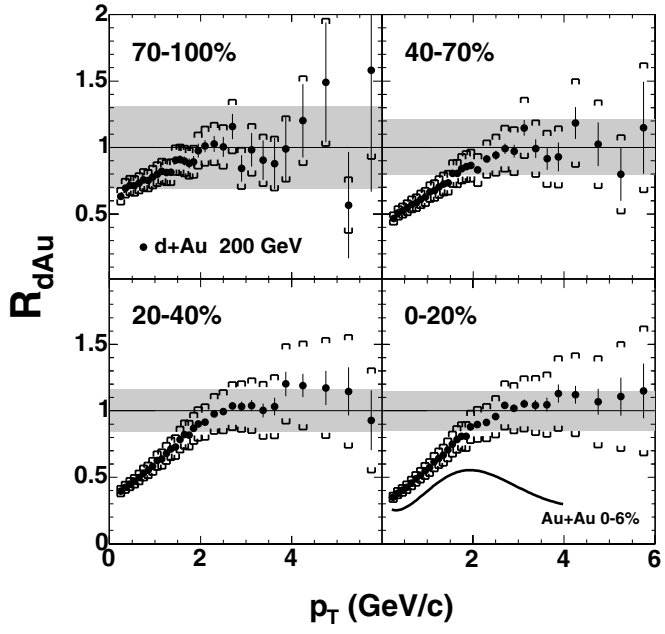

Fig. 1. Nuclear modification factor, R_{dAu}, as a function of transverse momentum for d+Au collisions at $\sqrt{s_{NN}}$ = 200 GeV, for four centrality ranges [7]. Centrality is expressed as a fraction of the total inelastic cross section, with smaller numbers being more central. Bars and brackets show statistical and systematic uncertainties, respectively. The shaded area shows the uncertainty (90 % C.L.) in R_{dAu} due to the systematic uncertainty in $N_{\rm coll}$ and the scale uncertainty in the proton-proton data. For comparison, the dark curve in the bottom right panel shows the nuclear modification factor, R_{AA}, for the 6 % most central Au+Au collisions at the same energy [26]

possible initial state effects. Calculations based on initial state effects were able to reproduce the observed magnitude of the high $p_{\rm T}$ suppression relative to the expectation of independent particle production [4].

In an effort to experimentally resolve the question as to whether the high $p_{\rm T}$ suppression was the result of initial state effects or the interaction of fast partons with the dense matter produced in Au+Au collisions, RHIC delivered deuteron-gold collisions. In d+Au, initial state effects for the nucleons in the deuteron traversing the Au nucleus are still expected to be present, whereas no dense matter is produced and therefore no final state suppression is expected [5]. The data are commonly shown in terms of the nuclear modification factor, R_{dAu}, defined as:

$$R_{dAu} = \frac{\sigma_{\rm p\overline{p}}^{\rm inel}}{\langle N_{\rm coll}\rangle} \frac{{\rm d}^2 N_{dAu}/{\rm d}p_{\rm T}{\rm d}\eta}{{\rm d}^2\sigma_{\rm p\overline{p}}/{\rm d}p_{\rm T}{\rm d}\eta} \quad . \qquad (1)$$

Consequently, an approach based on initial state saturation predicted a decrease in the nuclear modification factor R_{dAu} as a function of centrality by 25–30 % [4], whereas perturbative calculations predicted an increase in R_{dAu} by 15 % over the same centrality range [6], due to initial state $p_{\rm T}$ broadening.

The data on d+Au collisions [7–10] appear to provide an answer to this question, as shown in Fig. 1, from [7]. Unlike in Au+Au collisions, the charged hadron and neutral pion yields reach and exceed the binary collision scaling limit, showing that the observed high $p_{\rm T}$ suppression is indeed connected to the presence of the dense, hot medium produced in Au+Au collisions.

3 Identified hadron spectra in 200 GeV d+Au collisions

The spectra of positively charged hadrons produced in 200 GeV d+Au collisions [11] are presented in Fig. 2 as a function of transverse momentum (left) and transverse mass (right). Particle identification was performed using the PHOBOS Time-of-Flight detector. The data are averaged over all centralities (the average number of binary collisions is 9.7, due to the trigger bias of the online spectrometer trigger). These spectra are corrected for geometrical acceptance and tracking efficiency, the bias of the high-$p_{\rm T}$ trigger, and the finite momentum resolution of track reconstruction. Feed-down corrections for particles originating from weak decays have not been applied to these preliminary data. We estimate that this correction is less than 20 % even at the lowest transverse momentum, due to a strict cut on the distance between the collision vertex and the projected track origin.

We observe that the spectra for all particle species show a similar slope when plotted versus transverse mass. The pion and proton yields agree for a given $m_{\rm T}$ ("$m_{\rm T}$-scaling"), with the kaon spectrum about a factor of two lower. A strong violation of the transverse mass scaling was measured in Au+Au collisions [12,13], as a consequence of the strong radial flow that develops in heavy ion collisions.

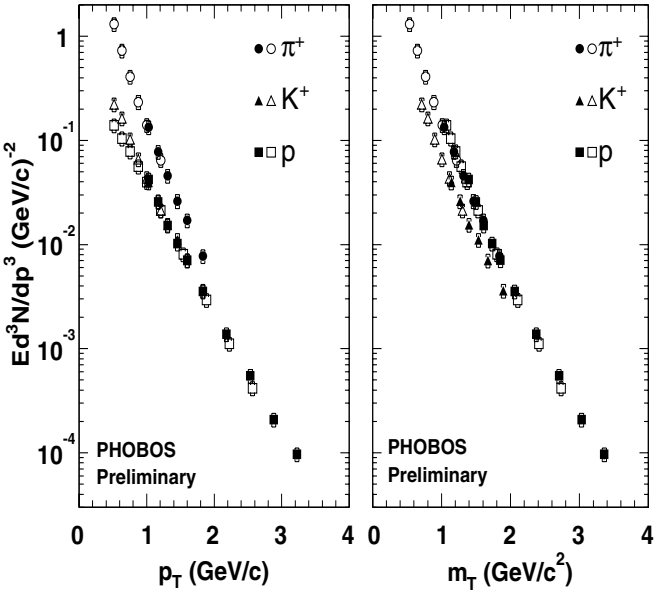

Fig. 2. Invariant yields of positive charged hadrons as a function of $p_{\rm T}$ (left) and $m_{\rm T}$ (right) in 200 GeV d+Au collisions. No feed-down correction was applied. Vertical bars show statistical and brackets show systematic errors

When dividing the d+Au data sample into three centrality bins (with average number of binary collisions of 5.6, 9.7, 14.5) we did not observe a significant variation in the particle composition of the transverse momentum spectrum.

4 Energy dependence of R_{AA}

In this section, we show data on the energy dependence of the high-$p_{\rm T}$ suppression seen in Au+Au data. Focusing first on central events, Fig. 3 shows the nuclear modification factor R_{AA}, defined in analogy to R_{dAu}, for the 6% most central Au+Au collisions at $\sqrt{s_{NN}} = 62.4$ GeV for four different values of $p_{\rm T}$ ranging from 1 to 4 GeV/c. Results from pp collisions at the same energy [14] were used in the calculation of R_{AA}. The 62.4 GeV results are compared with results for charged hadrons at $\sqrt{s_{NN}} = 130$ and 200 GeV. For $p_{\rm T} = 2$ GeV/c and above, we observe a smooth decrease of R_{AA} from 62.4 to 200 GeV in central Au+Au collisions.

Also shown in Fig. 3 is R_{AA} for π^0 production in Pb+Pb collisions at 17.2 GeV from WA98, obtained using three pp reference parametrizations [15–17], as well as π^0 data for 130 and 200 GeV from PHENIX [2,18]. The data indicate that R_{AA} for π^0 production at $p_{\rm T} > 3$ GeV/c drops from $R_{AA} > 1$ at $\sqrt{s_{NN}} = 17.2$ GeV to $R_{AA} < 0.2$ at $\sqrt{s_{NN}} = 200$ GeV, whereas the charged hadron pseudorapidity density over the same energy range changes by only a factor of two [19]. The data also show that, for the $p_{\rm T}$ range studied here, R_{AA} for neutral pions is consistently lower than for charged hadrons at the same collision energy.

5 Factorization of energy and centrality dependence

In the previous sections we have described separately the dependencies of a variety of observables on energy and centrality. In this section we will show that these two dependencies factorize to a remarkable extent.

One simple example of factorization was revealed by the PHOBOS measurements of the total charged particle multiplicity, $N_{\rm ch}$, divided by the number of pairs of participating nucleons in Au+Au collisions, at three energies from 19.6 to 200 GeV [20]. The normalized multiplicity was found to be independent of centrality for all energies.

A more striking example of factorization is shown in Fig. 4, where we plot the pseudorapidity density of charged particles per participant pair, near mid-rapidity, as a function of centrality, for collisions at 19.6 and 200 GeV [19]. Data for $\bar{\rm p}$p collisions at 200 GeV and interpolated to 19.6 GeV are also plotted. Over the centrality range shown here, the normalized yield at midrapidity in-

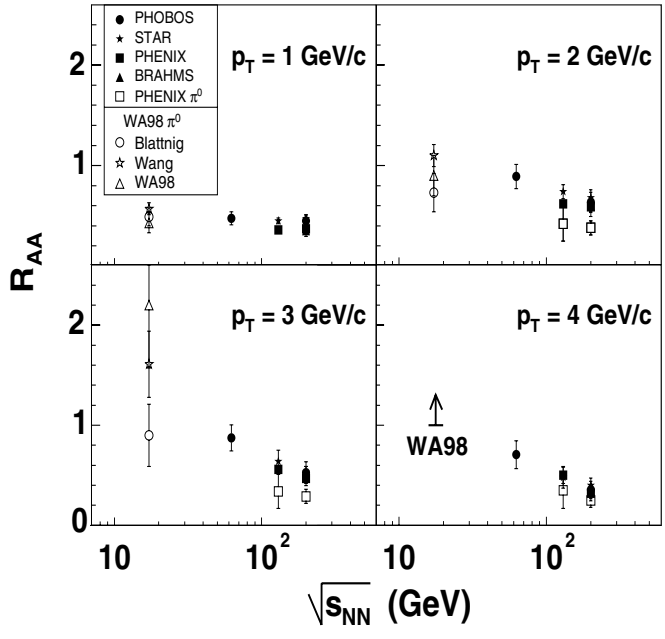

Fig. 3. Nuclear modification factor R_{AA} for central A+A events, as a function of collision energy for $p_{\rm T} = 1$, 2, 3 and 4 GeV/c. Filled symbols show data for charged hadrons, open symbols show π^0 data. For the WA98 π^0 data, R_{AA} is shown using three different parameterizations for the pp reference spectrum [15–17]; for $p_{\rm T} = 4$ GeV/c, the arrow indicates the lower limit on R_{AA}. The error bars show the combined systematic and statistical uncertainty obtained by interpolating the $p_{\rm T}$ dependence of R_{AA}

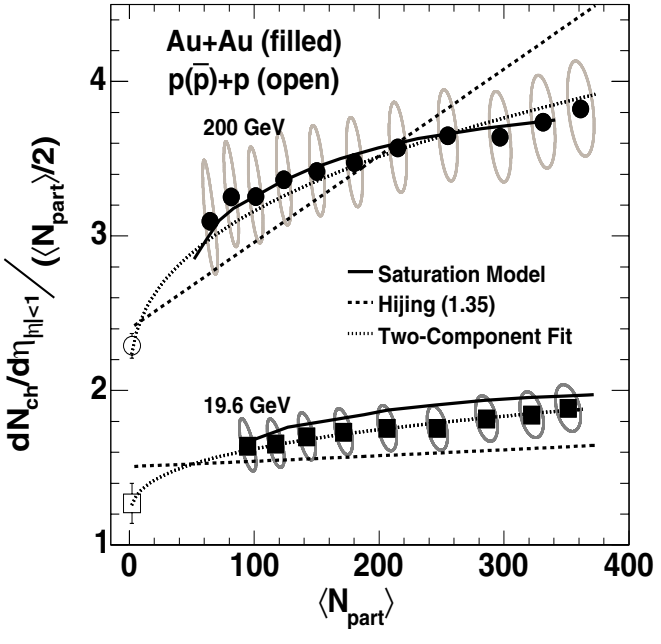

Fig. 4. Pseudo-rapidity density of charged particles emitted near midrapidity divided by the number of participant pairs as a function of the number of participants. Data are shown for Au+Au at collision energies of 19.6 and 200 GeV [19]. Data for pp or $\bar{\rm p}$p measured at 200 GeV and interpolated to 19.6 GeV are shown as open symbols [19]. The grey ellipses show the 90 % C.L. systematic errors. The results of two models [21–23] and one parameterized fit [29] are shown for comparison

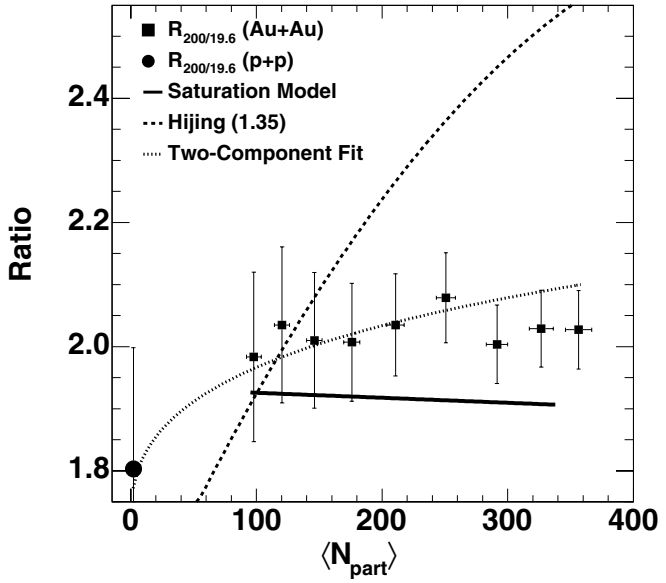

Fig. 5. Ratio of the pseudorapidity densities of charged particles emitted near midrapidity for Au+Au at 200 GeV over 19.6 GeV as a function of the number of participants [19]. The closed circle shows the ratio for collisions of protons. The error bars include both statistical and systematic errors. The ratios for the same two models and one fit shown in Fig. 4 are displayed for reference

creases by approximately 25 % from mid-peripheral to central collisions. Early theoretical explanations attributed this increase to the contribution of the hard component of particle production, which would grow with the relative increase in the number of binary nucleon-nucleon collisions in more central events. As an example of such a superposition of soft and hard particle production, the results of a HIJING calculation [21] are shown as dashed lines. The model shows an increase in the yield per participant pair, although steeper than that seen in the higher energy data.

However, this explanation is challenged by the detailed study of the energy dependence of mid-rapidity particle yields shown in Fig. 5, where the centrality dependence of the ratio of 200 to 19.6 GeV data is plotted [19]. Within the experimental uncertainty, this ratio is independent of centrality, whereas the contribution from hard processes would be expected to show a large increase over this collision energy range. This is illustrated by the HIJING prediction for this ratio (shown as a dashed line), which completely fails to capture the factorization of energy and centrality dependence for the midrapidity yield per participant. A similar result was found earlier (over a smaller span in beam energy) using the centrality dependence of normalized midrapidity yields from Au+Au at $\sqrt{s_{NN}} = 130$ GeV.

Also shown in Fig. 5 is the result of a saturation model calculation [22,23]. This model, which yields a reasonably good match to the energy evolution of particle yields at RHIC energies, also does a much better job of describing the centrality evolution than the HIJING model.

Another example of an energy-independent, non-trivial centrality dependence is seen in the comparison of charged hadron pseudo-rapidity distributions, when plotted in the approximate rest frame of one of the incoming nuclei, i.e. using the variable $\eta' \equiv \eta - y_{\rm beam}$. The distributions are found to agree over a broad range in η' [24].

Additional evidence for factorization is found in the transverse momentum distributions. In the absence of medium effects, one would expect that the volume scaling (i.e. proportionality to $N_{\rm part}$) observed for the bulk production of hadrons turns into scaling with the number of binary collisions ($N_{\rm coll}$) when measuring reaction products of point-like hard processes. This transition should be visible when studying particle production as a function of transverse momentum. As discussed earlier, particle production at large transverse momenta appears strongly modified in the presence of the medium produced in heavy ion collisions.

Data from the most recent RHIC run have been used to study the evolution of the transverse momentum distributions as a function of both collision centrality and energy. The measurements were performed near midrapidity at collision energies of 62.4 and 200 GeV [25].

It has been previously noted that the observed strong centrality dependence of R_{AA} at $\sqrt{s_{NN}} = 200$ GeV corresponds to a relatively small change in the yield per participating nucleon [26] between peripheral and central Au+Au collisions. These observation leads us to define

$$R_{AA}^{N_{\rm part}} = \frac{\sigma_{pp}^{\rm inel}}{\langle N_{\rm part}/2\rangle} \frac{{\rm d}^2 N_{AA}/{\rm d}p_{\rm T}{\rm d}\eta}{{\rm d}^2\sigma_{pp}/dp_{\rm T}{\rm d}\eta}, \qquad (2)$$

where we now scale the reference spectrum by $N_{\rm part}/2$, rather than $N_{\rm coll}$. The centrality, $p_{\rm T}$ and energy dependence of $R_{AA}^{N_{\rm part}}$ is shown in the middle row of Fig. 6 for collisions at 62.4 and 200 GeV. Over the range of $p_{\rm T}$ studied here, the yield per participant pair shows a variation of only $\approx 25\%$ from peripheral to central collisions for both collision energies.

This centrality independence is further illustrated in the bottom row of Fig. 6. The quantity $R_{PC}^{N_{\rm part}}$, defined as

$$R_{PC}^{N_{\rm part}} = \frac{\langle N_{\rm part}^{0-6\%}\rangle}{\langle N_{\rm part}\rangle} \frac{{\rm d}^2 N_{AA}/{\rm d}p_{\rm T}{\rm d}\eta}{{\rm d}^2 N_{AA}^{0-6\%}/{\rm d}p_{\rm T}{\rm d}\eta}, \qquad (3)$$

is shown as a function of $p_{\rm T}$ for the six centrality bins. $R_{PC}^{N_{\rm part}}$ measures the change in yield per participant pair, relative to a fit to the central data. Normalizing to the central, rather than the peripheral, data has the advantage that the results are more easily compared among different experiments with different ranges in centrality, while providing the same information in comparisons with theoretical calculations. Data are shown for collisions at 62.4 and 200 GeV. This plot again shows the small variation of the yield per participant pair from peripheral to central collisions. Furthermore, it demonstrates that the modification of the yield from peripheral to central collisions is the same for both energies, for $p_{\rm T}$ up to 4.5 GeV/c, within experimental uncertainties of less than 10 %. This striking

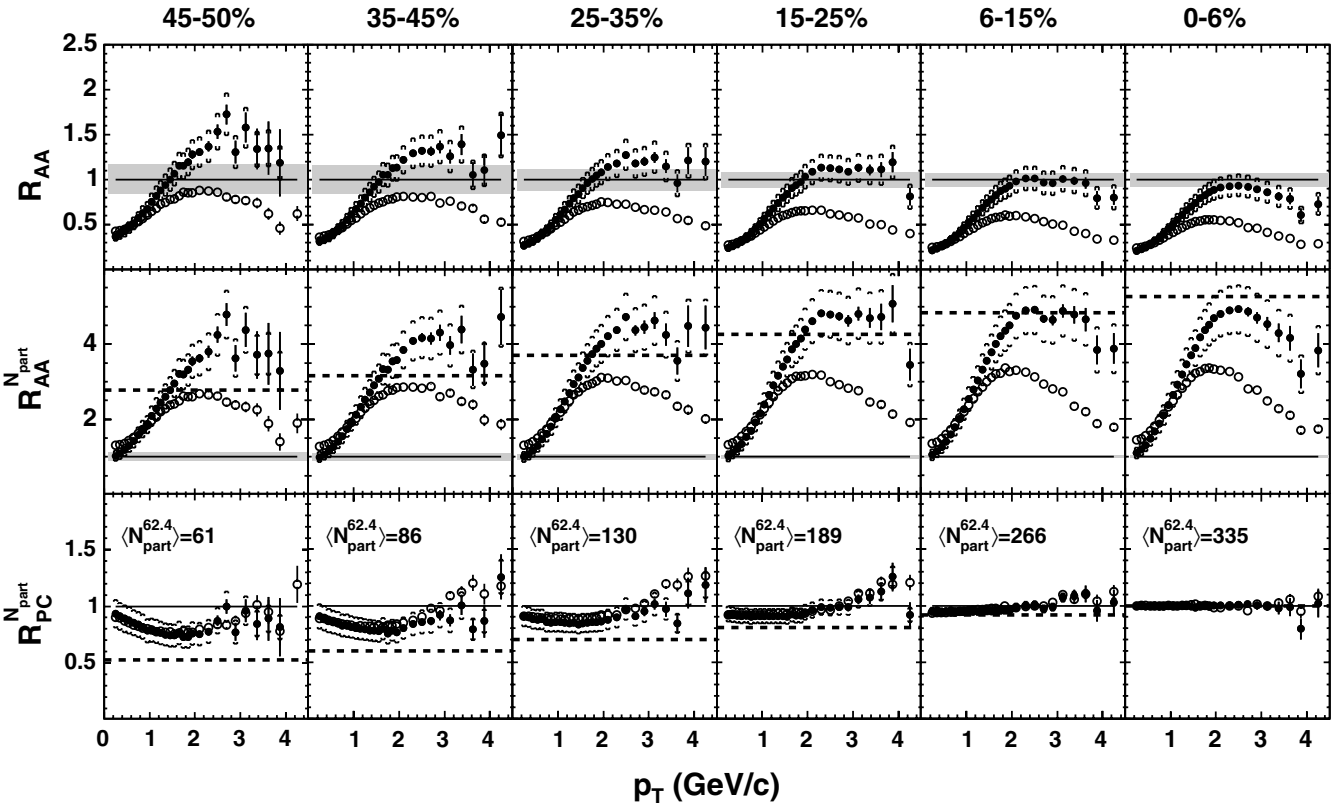

Fig. 6. Ratio of $p_{\rm T}$ distributions from Au+Au collisions to various reference distributions at $\sqrt{s_{NN}} = 62.4$ GeV (filled symbols) and 200 GeV (open symbols). Data are shown in six bins of centrality, ranging from $\langle N_{\rm part}\rangle = 61$ to 335 for 62.4 GeV collisions. The top row shows the nuclear modification factor R_{AA}, i.e. the ratio relative to proton-(anti)proton collisions scaled by $\langle N_{\rm coll}\rangle$. The grey band shows the uncertainty in $N_{\rm coll}$. The middle row shows $R_{AA}^{N_{\rm part}}$, which uses proton-(anti)proton spectra scaled by $\langle N_{\rm part}/2\rangle$. The bottom row shows $R_{PC}^{N_{\rm part}}$, using a fit to central data scaled by $\langle N_{\rm part}/2\rangle$ as a reference. The dashed line in the middle and bottom rows indicates the expectation for $\langle N_{\rm coll}\rangle$ scaling at $\sqrt{s_{NN}} = 62.4$ GeV relative to the reference distribution. Systematic uncertainties for all plots are shown by brackets (90 % C.L.)

agreement can be compared with the much larger variation of R_{AA} as a function of energy, centrality and $p_{\rm T}$.

Particle production at $p_{\rm T} > 1$ GeV/c in heavy-ion collisions is expected to be influenced by the interplay of many effects. This includes $p_{\rm T}$-broadening due to initial and final state multiple scattering (the 'Cronin effect'), the medium-induced energy loss of fast partons, and the effects of collective transverse velocity fields and of parton recombination [27]. The relative magnitude of these effects at 62.4 GeV is not yet known and will require further investigation. However, all these processes are expected to exhibit distinctly different dependences on collision energy and centrality. Yet, the results demonstrate, within the experimental uncertainties, a surprisingly clean factorization of the energy and centrality dependence of charged hadron yields in the intermediate $p_{\rm T}$-range studied here. This factorization of energy and centrality dependence is also a characteristic feature of total and differential particle yields [19,20] and of multi-particle correlation measurements such as Bose-Einstein correlations [28].

In summary, the PHOBOS results on high-$p_{\rm T}$ charged hadron spectra are consistent with the picture of a strongly-interacting medium being formed in Au+Au collisions. Furthermore, the observed factorization in the energy and centrality dependencies of transverse momentum spectra, combined with similar observations for total and mid-rapidity yields as well as the rapidity distributions, strongly suggests that the data reflect the dominant influence of yet-to-be-explained overall global constraints in the particle production mechanism in A+A collisions.

Acknowledgements. We acknowledge the generous support of the Collider-Accelerator Department at BNL for providing the 62.4 GeV beams. This work was partially supported by US DoE grants DE-AC02-98CH10886, DE-FG02-93ER40802, DE-FC02-94ER40818, DE-FG02-94ER40865, DE-FG02-99ER41099, W-31-109-ENG-38, US NSF grants 9603486, 0072204 and 0245011, Polish KBN grant 1-P03B-06227, and NSC of Taiwan contract NSC 89-2112-M-008-024.

References

1. B.B. Back et al. (PHOBOS), Nucl. Phys. A, arXiv:nucl-ex/0410022 (in press)
2. K. Adcox et al. (PHENIX), Phys. Rev. Lett. **88**, 022301 (2002)

3. M. Gyulassy, M. Plümer, Phys. Lett. **243**, 432 (1990)
4. D. Kharzeev, E. Levin and L. McLerran, Phys. Lett. **B561** (2003) 93.
5. X.-N. Wang, Phys. Rev. C **61**, 064910 (2000)
6. I. Vitev, Phys. Lett. B **562**, 36 (2003)
7. B.B. Back et al. (PHOBOS), Phys. Rev. Lett. **91**, 072302 (2003)
8. S.S. Adler et al. (PHENIX), Phys. Rev. Lett. **91**, 072303 (2003)
9. J. Adams et al. (STAR), Phys. Rev. Lett. **91**, 072304 (2003)
10. I. Arsene et al. (BRAHMS), Phys. Rev. Lett. **91**, 072305 (2003)
11. G. Veres (PHOBOS), J. Phys. G **30**, S1143 (2004)
12. S.S. Adler et al. (PHENIX), Phys. Rev. C **69**, 034909 (2004)
13. B.B. Back et al. (PHOBOS), Phys. Rev. C **70**, 051901(R) (2004)
14. A. Breakstone et al., Z. Phys. C **69**, 55 (1995); 55; D. Drijard et al., Nucl. Phys. B **208**, 1 (1982)
15. M.M. Aggarwal et al., Eur. Phys. J. C **23**, 225 (2002); M.M. Aggarwal et al., Phys. Rev. Lett. **81**, 4087 (1998); Erratum-ibid. **84**, 578 (2000)
16. X.-N. Wang, Phys. Rev. Lett. **81**, 2655 (1998); E. Wang, X.-N. Wang, Phys. Rev. C **64**, 034901 (2001)
17. D. d'Enterria, Phys. Lett. B **596**, 32 (2004)
18. S.S. Adler et al. (PHENIX), Phys. Rev. Lett. **91**, 072301 (2003)
19. B.B. Back et al. (PHOBOS), Phys. Rev. C **70**, 021902(R) (2004)
20. B.B. Back et al. (PHOBOS), arXiv:nucl-ex/0301017
21. M. Gyulassy, X.-N. Wang, Comput. Phys. Commun. **83**, 307 (1994); HIJING v1.383 used for d+Au, and v1.35 used for Au+Au
22. D. Kharzeev, E. Levin, Phys. Lett. B **523**, 79 (2001)
23. D. Kharzeev, E. Levin, M. Nardi, arXiv:hep-ph/0111315
24. B.B. Back et al. (PHOBOS), Phys. Rev. Lett. **91**, 052303 (2003)
25. B.B. Back et al. (PHOBOS), Phys. Rev. Lett. **94**, 082304 (2005)
26. B.B. Back et al. (PHOBOS), Phys. Lett. B **578**, 297 (2004)
27. For a recent review, see P. Jacobs, X.-N. Wang, Prog. Part. Nucl. Phys. **54**, 443 (2005)
28. D. Adamova et al. (CERES), Nucl. Phys. A **714**, 124 (2003)
29. D. Kharzeev, M. Nardi, Phys. Lett. B **507**, 121 (2001)